Science Translational Medicine
AAAS

Supplementary Materials for

Metabolic modulation of synaptic failure and thalamocortical hypersynchronization with preserved consciousness in Glut1 deficiency

Karthik Rajasekaran *et al.*

Corresponding author: Juan M. Pascual, juan.pascual@UTsouthwestern.edu

Sci. Transl. Med. **14**, eabn2956 (2022)
DOI: 10.1126/scitranslmed.abn2956

The PDF file includes:

Other Supplementary Material for this manuscript includes the following:

SUPPLEMENTARY METHODS

EEG and prandrial dependence of the EEG

EEG acquisition and overall analysis

Standard clinical scalp EEG recordings were obtained from G1D individuals using a medical XLTEK digital EEG system. A 10-20 and modified combinatorial nomenclature system of electrode placement with bipolar referencing was used with the addition of FT9 and FT10 electrodes (referred to as in standard EEG nomenclature) and two EKG electrodes. The recordings were imported into Natus NeuroWorks EEG software for archiving, offline review, average referencing (using the software) and analysis. A notch 60 Hz filter was applied. The voltage changes (in μV) thus recorded by 25 electrodes were compiled in a spreadsheet for further analysis, which utilized MATLAB with standard available functions and scripts. To avoid frontal eye field motion artifacts and given its relative proximity to the somatomotor cortex, channel P3, overlying the left parietal lobe was selected for analysis. The unprocessed EEG from P3 was visualized over sequential time segments of 30 s. Spectrogram and continuous wavelet transform (CWT)/ magnitude scalogram plots along with the unmodified EEG signal were scrutinized to observe the time-frequency characteristics of the EEG signal. Putative epileptiform events were selected for further analysis.

Prandial dependence

Individuals were hospitalized specifically for this study and provided with their habitual, non-therapeutic meals (which were non-ketogenic and contained each participant's normally preferred nutrient composition and caloric value) at habitual mealtimes during the course of 23 hr. There was no noticeable deviation from habitual caloric content or schedule. Previous anticonvulsant medication use was not modified and varied substantially. Time segments comprising 2 hr prior to a meal and 1 hr following a meal were further analyzed for all the participants. The first 1 hr of the 23 hr-long recording was omitted from analysis due to motion artifact during electrode placement in some of the recordings.

Epileptiform event analysis

Potential epileptiform events were divided into 1 s segments. A power spectral density (PSD; a measure of power with respect to EEG signal frequency), was generated for each 1 s segment using fast Fourier transform. The average power spectra of the 1 s segments was converted into logarithmic scale. For each individual, 100 30-s segments were chosen at random from the non-epileptiform areas of the EEG. These 30 s segments too were divided into 30 1-s segments and average PSDs were generated as described for epileptiform events. Baseline correction was performed on each epileptiform event as a part of pre-processing to eliminate any background activity. This was accomplished by subtracting the averaged PSD of the 100 random (non-epileptiform) segments from the average PSD of the epileptiform event. The baseline corrected PSD was plotted for every event and the prominent peak frequency was noted using MATLAB function *findpeaks*. A seizure rate, defined as the total cumulative duration of all epileptiform events divided by the total duration the EEG analyzed was computed, and this computation was applied before meal consumption (preceding 2 hr) and after meal consumption (subsequent 1 hr) where indicated.

Source localization of the EEG

Participant selection

A total of 81 seizures were selected from 6 individuals recruited as above. The distribution of ages (in years) was 2-19. Brain dimensions were accounted for by normative head circumference – brain size relations. G1D individual head circumferences were contrasted age-normal values for the estimation of microcephaly that often occurs in in G1D using normal head circumference estimates for a racially mixed population comparable to the G1D individuals. The individuals received 21-channel EEG monitoring continuously with each episode analyzed lasting from 2 to 5 min.

Source localization method

To perform electrical source reconstruction, each participant was matched to a brain anatomical template T1 MRI from a public database (*79*). Matching was based on age and templates were rescaled according to the head circumference of each individual. Electrode positioning followed the 10-

10 International System with references at auricular points. Further data analysis was performed with Brainstorm (*80*). Template MRI were segmented on scalp, skull and cortex using SPM (*81*). A forward distributed dipole model was created over the MRI space using OpenMEGG (*82, 83*). The forward model was employed to estimate the magnitude of distributed dipoles by using sLORETA (*84*). The magnitude of distributed dipoles was indicative of activity over an area of the brain. Template MRI were further segmented using SPM into the regions indicated by LPA40 atlas (*85*). For the baseline (pre-seizure) period and for each of the 5 seizure sequential 20% time segments, we presented the activity patterns of current density in accumbens, amygdala, caudate, cerebral cortex, cerebral white matter, hippocampus, lateral ventricle, pallidum, putamen, thalamus, ventral diencephalon further divided into left and right. Several regions of interest were selected in the cortex, including frontal, pre-motor, somatosensory, parieto-occipital, visual and temporal cortex (again separated into left and right) and we compared their activity elevations during the same 20% temporal seizure segments to estimate the sequence of activation among cortical regions. The total activity in each brain region was computed by adding the magnitudes of all dipoles within each region and then dividing by the volume of the given region.

EEG data processing

Each of the seizure time segments was first divided into 5 equal-sized sub-segments to account for time variability during an ictal episode. For baseline comparison, each seizure segment was matched with a vicinal segment of equal length but with no ictal activity prior to the seizure and this was considered the baseline segment. Each segment (0-20%, 20-40%, 40-60%, 60-80% and 80-100%) accounted for one fifth of the seizure period. Although the length of each seizure episode varied, we standardized the data sets by considering the time-average activities over each period. Total activity was then computed for the ictal segments over each brain region of interest and averaged over all sub-segments. Baseline segments received the same treatment using the complete segment instead of sub-segments. To mitigate the effects of area and location differences, the total activity of each

segment and region was divided by the total activity over the same region in the baseline matched segment to yield the elevated activities during seizure over the baseline.

Human brain ^{18}F-DG PET

6 genetically confirmed 16–39-year-old G1D individuals free of other diseases were studied via ^{18}F-FDG PET. 0.15 μCi/Kg ^{18}F-deoxy-glucose (FDG) was intravenously injected following a 8 hr fasting period except for water. Basal (fasting) glucose was normal for all individuals, measuring <100 mg/dl. PET images obtained in a clinical Siemens ECAT EXACT HR scanner (nominal resolution power 4 mm) were acquired during a 60 min period that followed injection by 30 min. The standard clinical radiological procedure included multiframe technique and auto attenuation correction, dynamic scan mode (4 frames at 480 s/frame) and filter back projection. Reconstruction with auto attenuation correction employed a Hann filter (cut-off 0.40 cycles/pixel). Regions of interest were manually selected to include 2.53 mm (transverse image thickness) × 1 cm (lateral dimension) × 1 cm (posteroanterior dimension). For comparison, 4 normal 19-36-year old individuals were also studied.

EEG-fMRI

Traditionally, it has proven difficult to directly correlate simultaneously recorded EEG and fMRI data on a single-individual, because single-trial EEG data are noisy and signal recorded on an electrode reflects a summation of incoherent neural activity across a large brain region (*86*). In this case, our data reliability benefited from the coherent and high-amplitude spike-wave discharge in the EEG recording (**Fig. 1A**). The prolonged ~2-4 Hz discharges typical of G1D, which often last over 10 s, provide an opportunity to accurately map the evolution of seizure activity using EEG-fMRI by overcoming these limitations and to identify functional anatomy of G1D seizures (*87*).

G1D individuals 19-31 years old, male and female genetically diagnosed with G1D were studied on a Philips 3T MRI scanner (Philips Healthcare, Best, The Netherlands). The participants were fitted with a 32-channel MRI compatible EEG cap (Brain Vision, Morrisville, USA) before entering the MRI scanner. Once a participant was placed inside the MRI, EEG signals were recorded for 15 min while

blood-oxygenation-level-dependent (BOLD) functional MRI data were continuously collected. Participants were instructed to stay awake and still inside the MR scanner without performing any specific tasks. The imaging parameters of the BOLD fMRI were: voxel size 3.44 x 3.44 x 5mm^3, 29 slices covering the entire brain, TR/ TE/ flip angle= 1500ms/ 30ms/ 60°. For anatomical reference, a high resolution structural scan (T1-weighted) was also obtained and the scan time was 4 min. For analysis of the EEG data, spurious signals induced by the MRI gradients, cardiac pulsation, and eye blinking were removed (Brain Vision Analyzer 2.0, Morrisville, USA). Next, the onset time and duration of each seizure event were identified manually by marking the spike waves on the EEG time course, which were quite characteristic (**Fig. 3A** and **D**). For the fMRI data, pre-processing included motion correction, image registration, and normalization to the Montreal Neurological Institute brain template. Then, a linear regression analysis was performed in which the seizure time course determined from the EEG data was used as the independent variable and voxel-wise BOLD time course was the dependent variable. A voxel-wise general linear regression analysis was performed in which the time course of seizure occurrence (0 for non-seizure time points and 1 for seizure time points) was the independent variable and the voxel-wise BOLD fMRI time course was the dependent variable. Motion vectors as well as the white matter and CSF time courses were also included as additional regressors in the model to ensure that the activation/deactivation patterns observed are not due to participant motion and global signal fluctuations. Seizure-activated voxels were identified based on a voxel-specific threshold of $p < 0.001$ and a cluster size of 200 voxels.

Mouse ^{18}F-DG PET

7 4 – 5 month old G1D and 7 littermate control male mice were fasted for 2 hr and administered 0.25 ml containing a ^{18}F-deoxyglucose dose of 1.5 µCi/ g of body weight diluted in saline solution via tail vein injection following anesthesia with ketamine and xylazine. The mice were immediately scanned for 1 hr in a Siemens Inveon PET/CT Multimodality System for laboratory animals with nominal resolution 1.4 mm. A manually delineated region of interest encompassed the entire brain or the entire liver aided by superimposition of associated CT images.

Brain glycogen determination

4 control and four G1D 14-week-old mice animals were prepared using standard histological methods for immunohistochemical staining with the anti-glycogen IV58B6 antibody and amyloglucosidase-based glycogen assays were also used to determine regional and total glycogen abundance as described (*88*). HALO software (Indica Labs, Albuquerque, NM) was employed to quantify and the enzymatic glycogen determination was measured with a spectrophotometric microplate reader.

^{13}C mass spectrometry

A set of G1D (n =9) and normal (n= 9) forebrains was collected after conscious decapitation and flash-freezing on dry ice (brain dissection time <15 s) according to standard procedures validated at the Metabolic Mouse Phenotyping Center at Case Western University (MMPC) and shipped to the MMPC for chromatography mass spectrometry (GC-MS/LC-MS) and characterization of acetyl-coenzyme A and other metabolites as previously described (*18*). **Datafile S2** details the use of each mouse in the assays.

Electrophysiology

Animals were anesthetized with isoflurane prior to decapitation. Brains were dissected free and immersed in cold (2-4°C) ACSF containing (in mM) 5.5 NaCl, 2 KCl, 5 $MgSO_4$, 1.1 KH_2PO_4, 1 $CaCl_2$, 20 glucose, 25 $NaHCO_3$, 113 sucrose saturated with 95%O_2-5%CO_2. Brains were mounted on a vibratome stage (Leica VT1000S vibroslicer) and 300 µM thick horizontal sections cortical and thalamic slices. Slices were maintained in continuously oxygenated ACSF containing (in mM) 127 NaCl, 2 KCl, 1.5 $MgSO_4$, 1.1 KH_2PO_4, 1.5 $CaCl_2$, 20 glucose, 25.7 $NaHCO_3$ at 32°C in a holding chamber for 30-45 min and then maintained at room temperature for the next 6-8 hrs. For patch clamp recordings, slices were placed in a recording chamber mounted on the stage of a Scientifica microscope equipped with a 40x water-immersion objective, IR-DIC optics, and video. All recordings were performed at 32°C. Patch electrodes (final resistances 3-4 MΩ were pulled from borosilicate glass (Sutter Instruments, Novato,

CA) on a horizontal Flaming-Brown microelectrode puller (model P-1000, Sutter Instruments), using a 2-stage pull protocol. To record inhibitory synaptic currents, recording electrodes were filled with a filtered internal recording solution consisting of (in mM): CsCl 153.3, $MgCl_2$ 1.0, N-[2-Hydroxyethyl] piperazine-N -[2-ethansulfonic acid] (HEPES) 10.0, and glycol-bis (α-aminoethyl ether) N,N,N ,N - tetraacetic acid (EGTA) 5.0, pH 7.2 (with CsOH), osmolarity was 285-295 mOsm. Neurons were voltage-clamped to -65 mV with an HEKA10 amplifier (Harvard Bioscience). To record excitatory postsynaptic currents (EPSCs), patch electrodes (final resistance 3 - 6 MΩ) were filled with a filtered internal recording solution consisting of (in mM): 117.5 $CsMeSO_4$, 10 2-Hydroxyethyl] piperazine-N - [2-ethansulfonic acid] (HEPES), 0.3 N-[and glycol-bis (a-aminoethyl ether) N,N,N,N -tetraacetic acid (EGTA), 15.5 CsCl, and 1.0 $MgCl_2$, pH 7.3 (with CsOH); the osmolarity was 290-300 mOsm. Electrode shank contained 5 mM QX-314 to block voltage gated sodium channels. Recordings, both excitatory and inhibitory were generally performed at a holding potential of -65 mV if series resistance after compensation was 20 MΩ or less. Access resistance was monitored with a short hyperpolarizing test pulse every 10 minutes. If the series resistance increased by 25% at any time during the experiment, then the recording was terminated. Currents were filtered at 3.5 kHz, digitization was accomplished by the digitizer built into the amplifier and acquired using Patchmaster 10 software (HEKA/Harvard Bioscience, CA) using a Windows 7 computer. An adaptive noise cancelling Humbug device was included in most voltage clamp studies (except tonic inhibition). Current clamp recordings were performed using a recording solution containing (in mM) 100 potassium gluconate, 5 KCl, 10 HEPES, 1 EGTA, 2 $MgCl_2$, 0.1 $CaCl_2$, pH 7.2. Electrode shank contained 0.5 mM ATP Mg^{2+} salt.

To record inhibitory synaptic currents, the bath solution also contained 50 μM DL-2-Amino-5-phosphonopentanoic acid (DL-AP5) and 20 μM 6-Cyano-7-nitroquinoxaline-2,3-dione (CNQX, Tocris-Cookson) to block glutamatergic currents. Alternatively, to block GABAergic currents when obtaining excitatory currents, slices were perfused with GABAergic antagonists, picrotoxin or bicuculline (100 μM). Tonic inhibition studies were performed in the presence of 10 μM of the GABA uptake inhibitor, NO-711 (Sigma). Miniature postsynaptic currents were obtained from cortical slices perfused with 1 μM

tetrodotoxin (Tocris). Synaptic currents were analyzed using MiniAnalysis software. Tonic currents and current clamp studies were analyzed using Clampfit 10.

Pilocarpine-induced generalized tonic clonic seizures (GTCS)

G1D and control mice were injected with varying doses pilocarpine to obtain dose response curves to determine their respective ED50 values. Experiments were then performed in all animals with pilocarpine (27 mg/kg intraperitoneally) and monitored continuously for behavioral GTCS that were scored behaviorally from video recordings as per Racine criteria (*36*). The efficacy of drugs on terminating early and late GTCS (established status epilepticus; SE) was studied by intervening at 2 time points, t1 (<1 minute following seizure onset), or t2 (established phase, at 30 min following seizure onset). Seizure termination was defined as the absence of behavioral convulsions, myoclonus and freezing and staring activity over a 3 hr observation period following drug administration. Acute EEG data were obtained from G1D animals: Bipolar insulated stainless steel electrodes were implanted stereotaxically over the hippocampus and cortex of the animals and they were allowed to recover for 5 – 7 days. After the recovery period, SE was induced by administration of pilocarpine and seizures were monitored for 5 hours by video-EEG using a MATLAB integrated TDR system. Seizure onset was characterized by continuous electrographic spike wave and polyspike discharges with a frequency greater than 2 Hz and amplitude at least 3 times that of the baseline. SE was considered terminated when the EEG returned back to baseline and spiking activity was arrhythmic and below 2 Hz during a 3 hr monitoring period. The EEG criterion for status epilepticus was the occurrence of continuous epileptiform activity for 30 minutes during which spike frequencies did not drop below 1 Hz or intermittent seizures lasting 30 minutes with brief periods of spiking lasting less than 5 min. The termination of these events was recorded when the spike frequency dropped below 1 Hz for more than 30 min. EEG data were analyzed with a custom written MATLAB software and a blinded investigator analyzed the data, including total power spectrum analysis and time to seizures, and seizure remission and recurrence over a 24 hr period.

SUPPLEMENTARY FIGURES

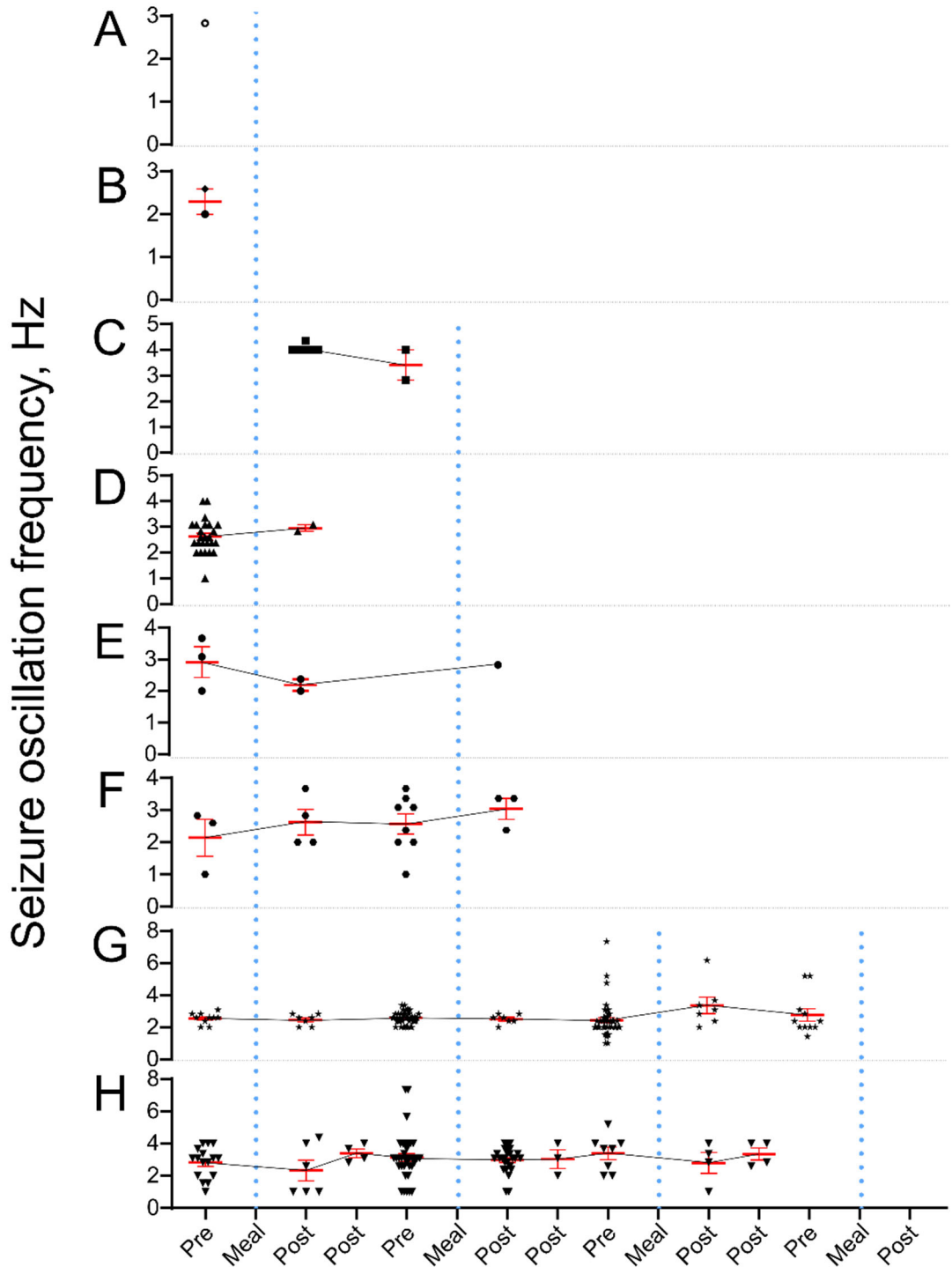

Supplementary figure 1. Oscillatory periodicity in G1D seizures in relation to meal times. A-H: oscillation frequency for all seizures recorded from 8 G1D individuals consecutively recruited and studied during 23 hr from 12 pm to 11 am the next day. When seizures were present in a pre or post meal interval, their oscillatory periodicity is noted in red as mean ± s.e.m. Meal times (vertical dotted blue lines) were approximately homogeneous for all participants. Meals were chosen by the individuals from their habitual non-therapeutic dietary repertoire. Paired *t*-tests for oscillatory frequency variation in each of participants C to H showed no significant differences ($p > 0.05$).

[**Supplementary figure 2** below continues on the next 5 pages]

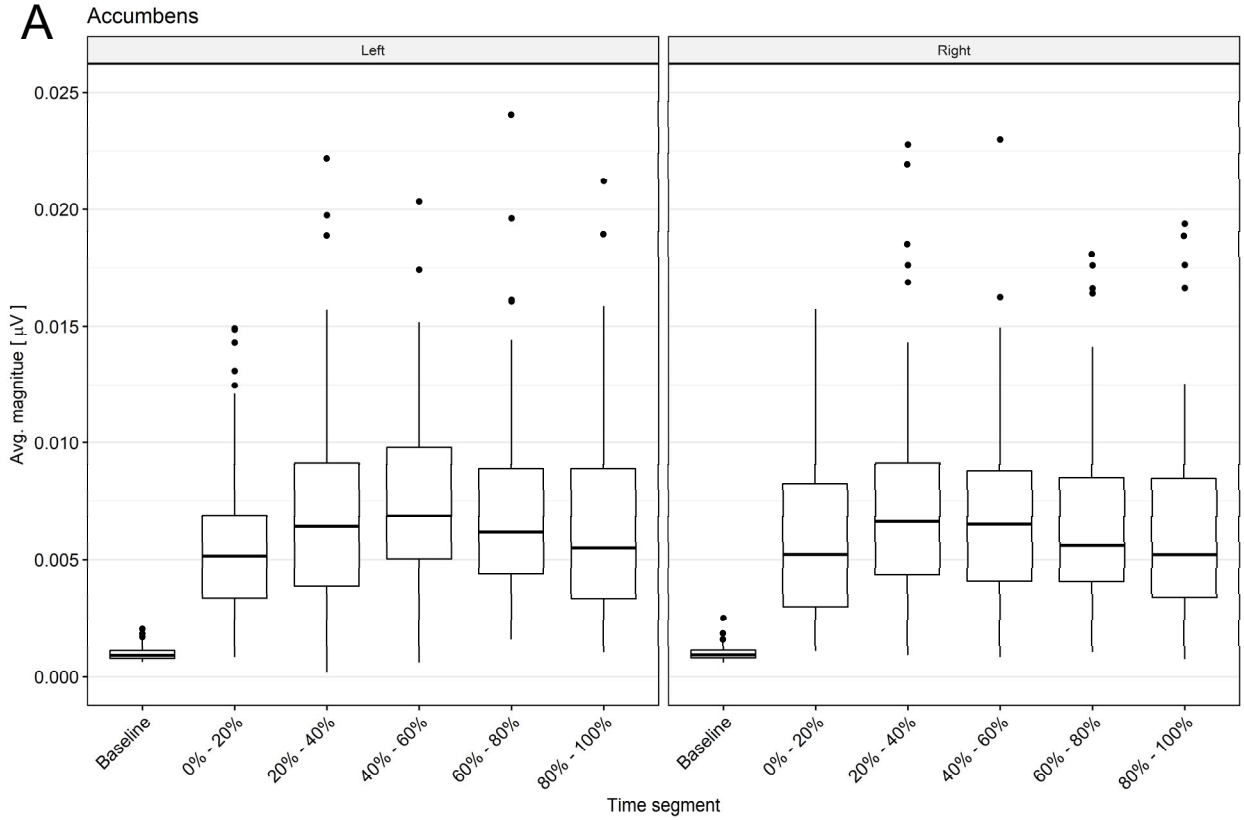

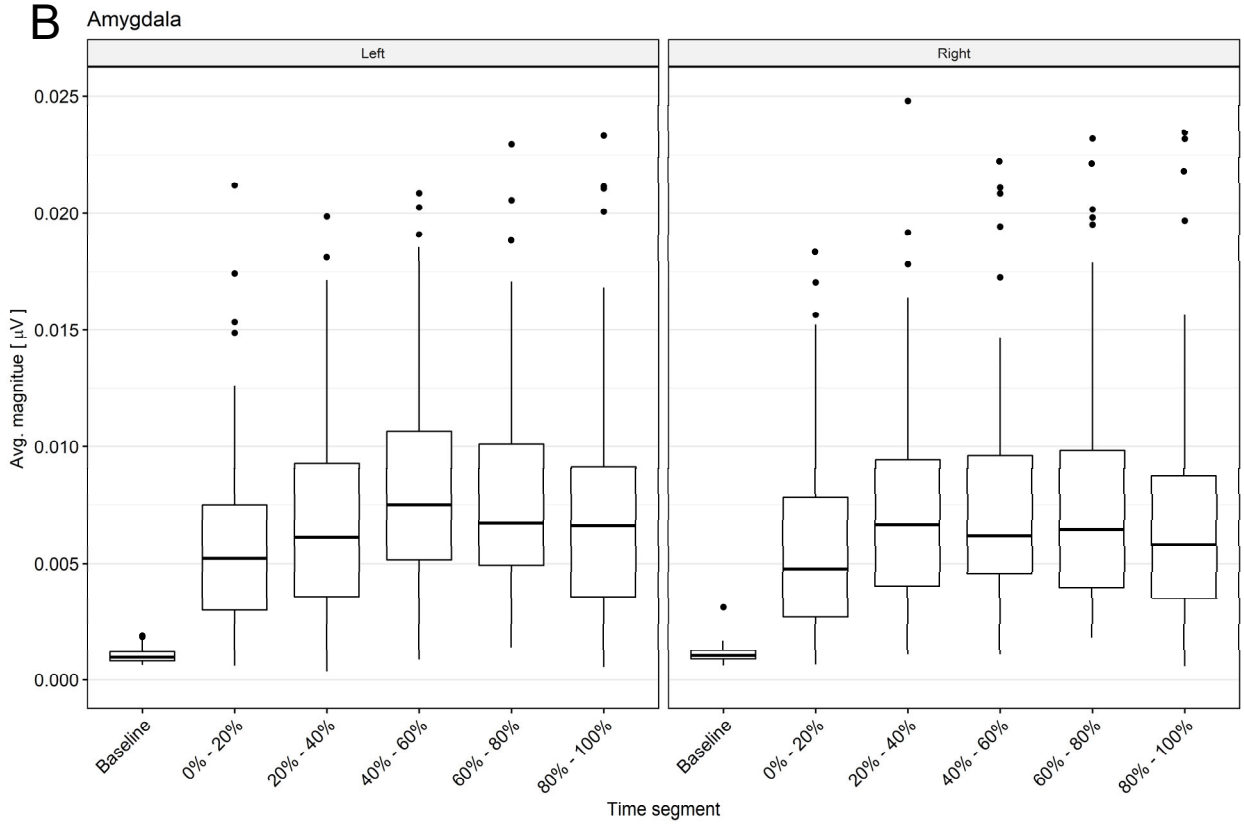

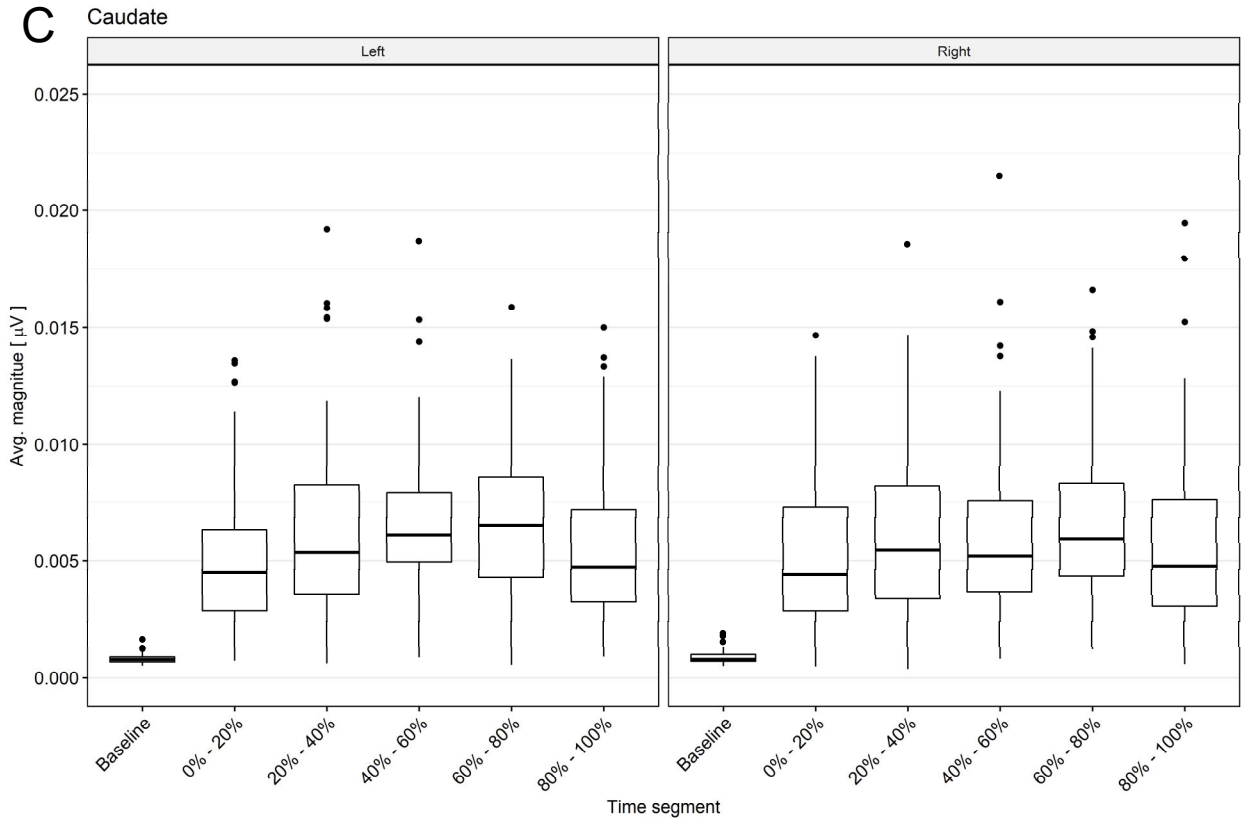
C
Caudate
Left
Right
0.025
0.020
0.015
0.010
0.005
0.000
Avg. magnitue [µV]
Baseline
0% - 20%
20% - 40%
40% - 60%
60% - 80%
80% - 100%
Time segment

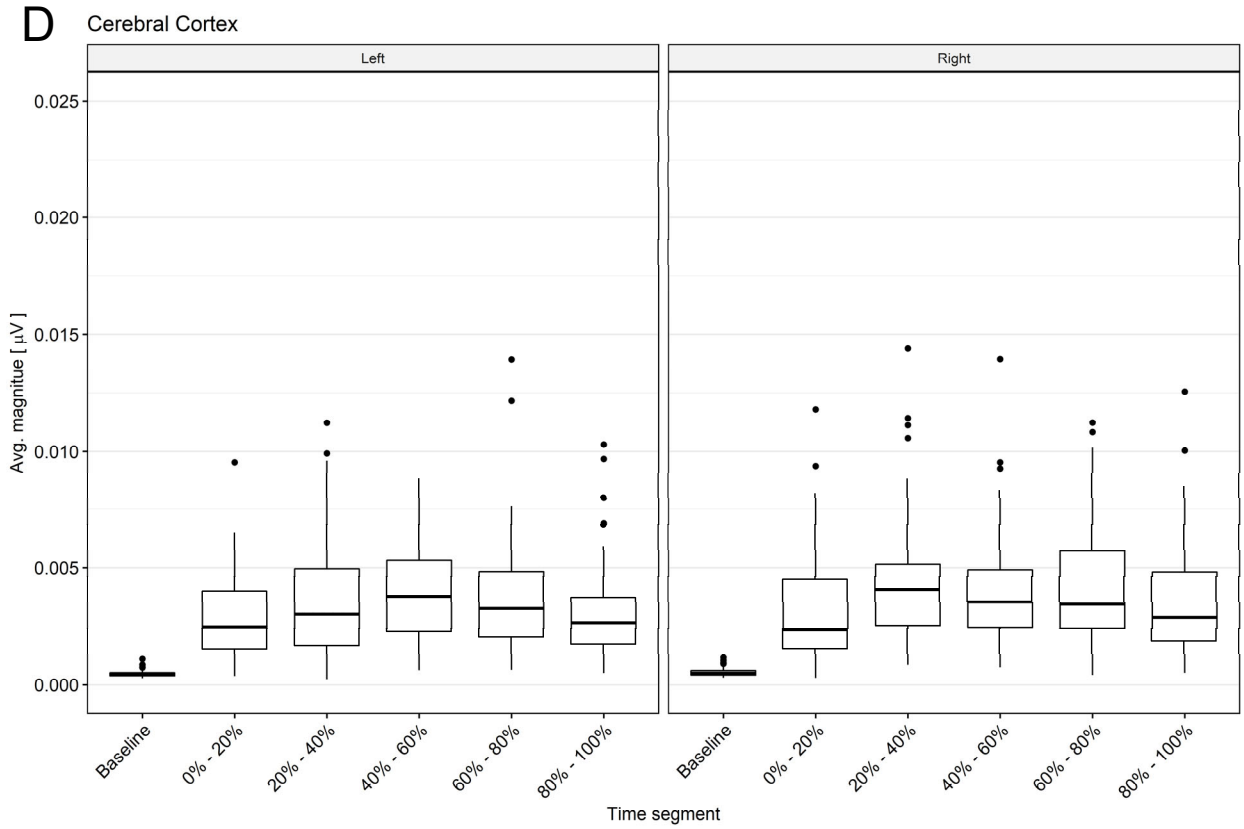
D
Cerebral Cortex
Left
Right
0.025
0.020
0.015
0.010
0.005
0.000
Avg. magnitue [µV]
Baseline
0% - 20%
20% - 40%
40% - 60%
60% - 80%
80% - 100%
Time segment

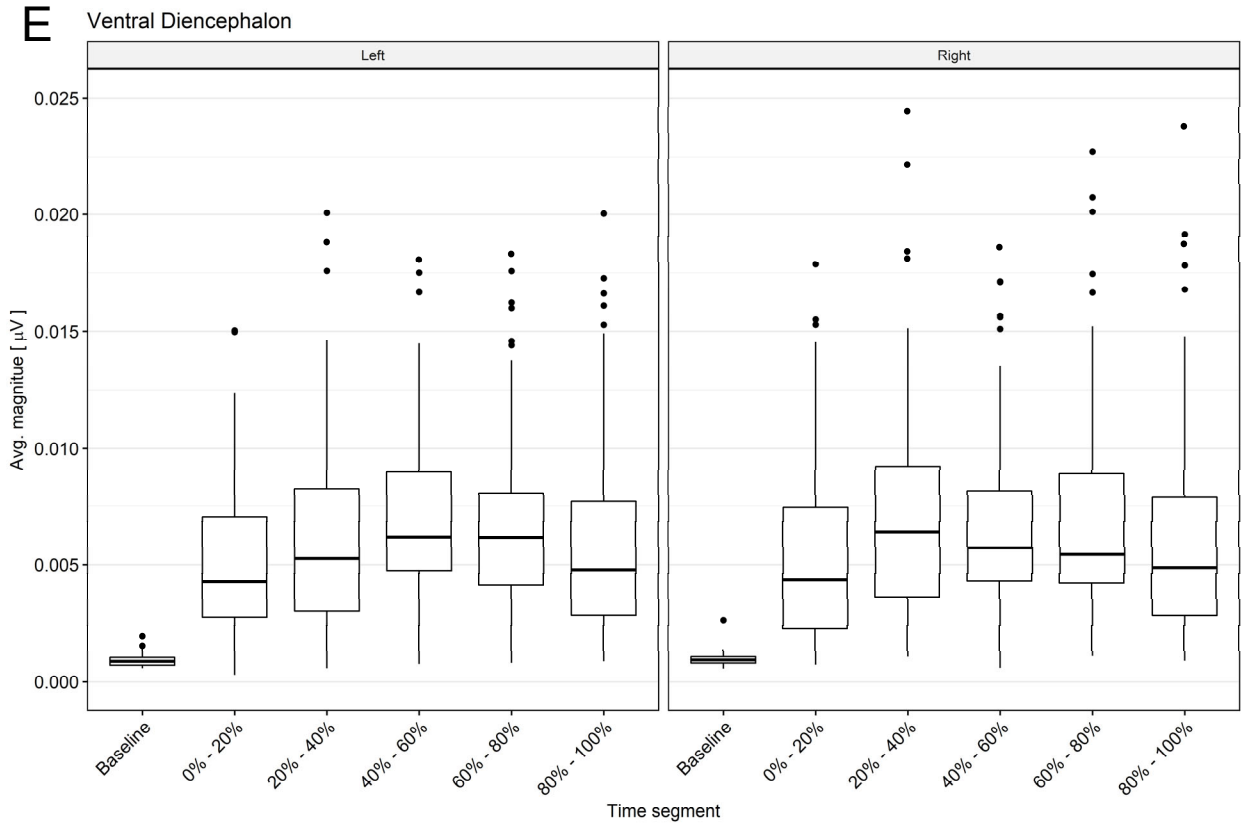
E
Ventral Diencephalon
Left
Right
Avg. magnitue [µV]
0.025
0.020
0.015
0.010
0.005
0.000
Baseline
0% - 20%
20% - 40%
40% - 60%
60% - 80%
80% - 100%
Time segment

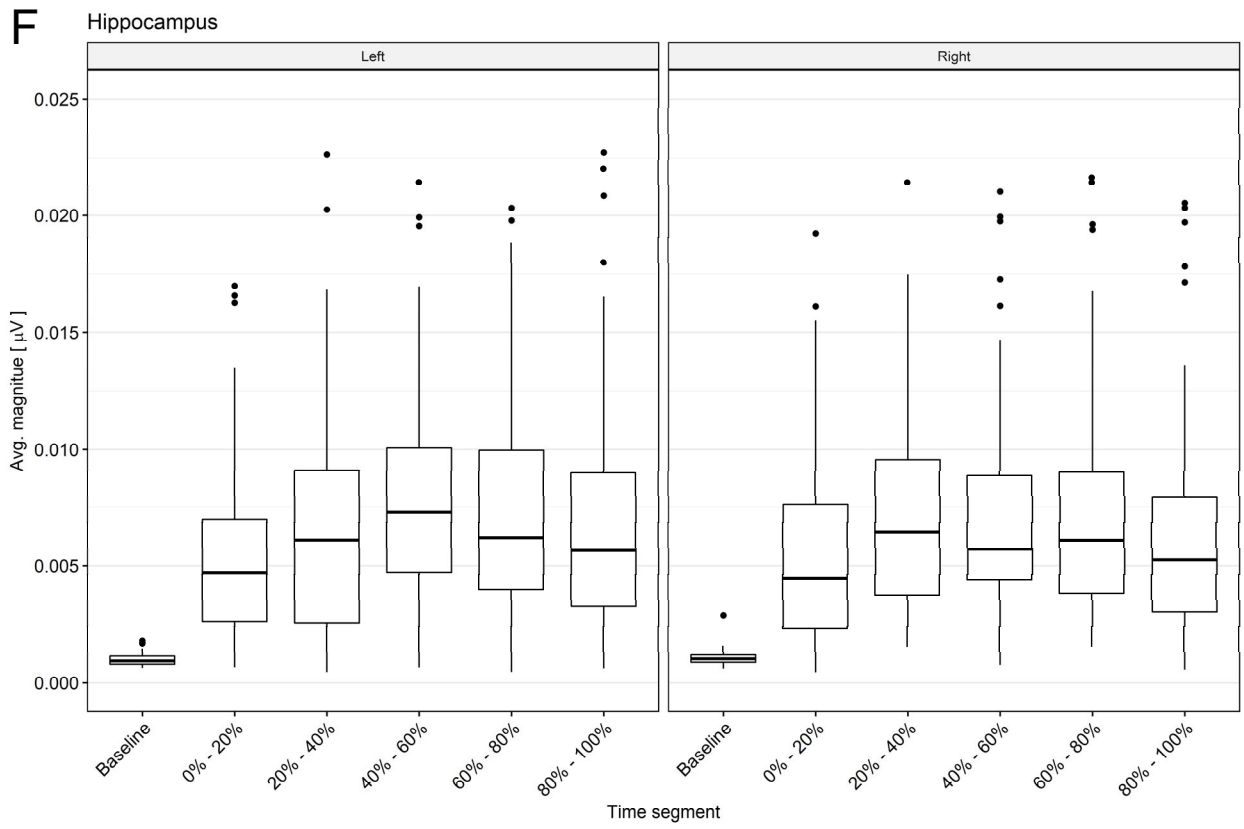
F
Hippocampus
Left
Right
Avg. magnitue [µV]
0.025
0.020
0.015
0.010
0.005
0.000
Baseline
0% - 20%
20% - 40%
40% - 60%
60% - 80%
80% - 100%
Time segment

G Pallidum

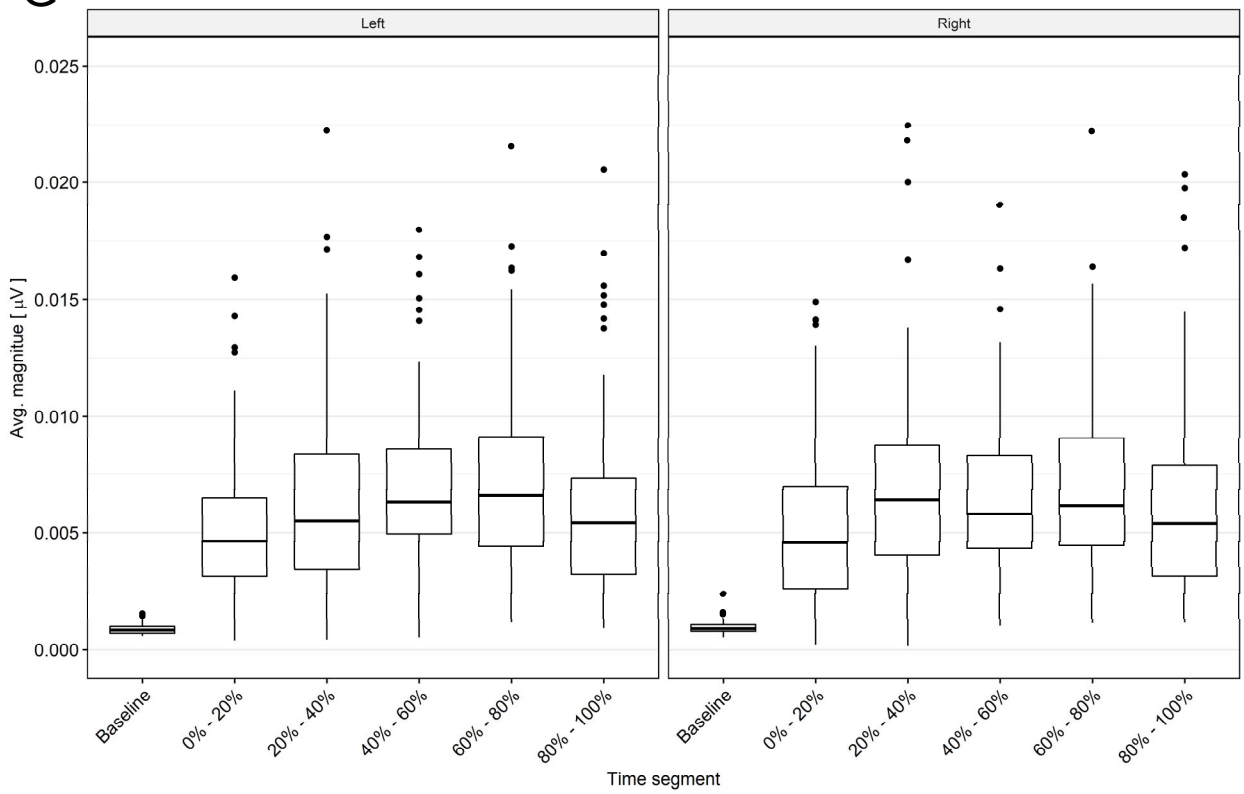

H Putamen

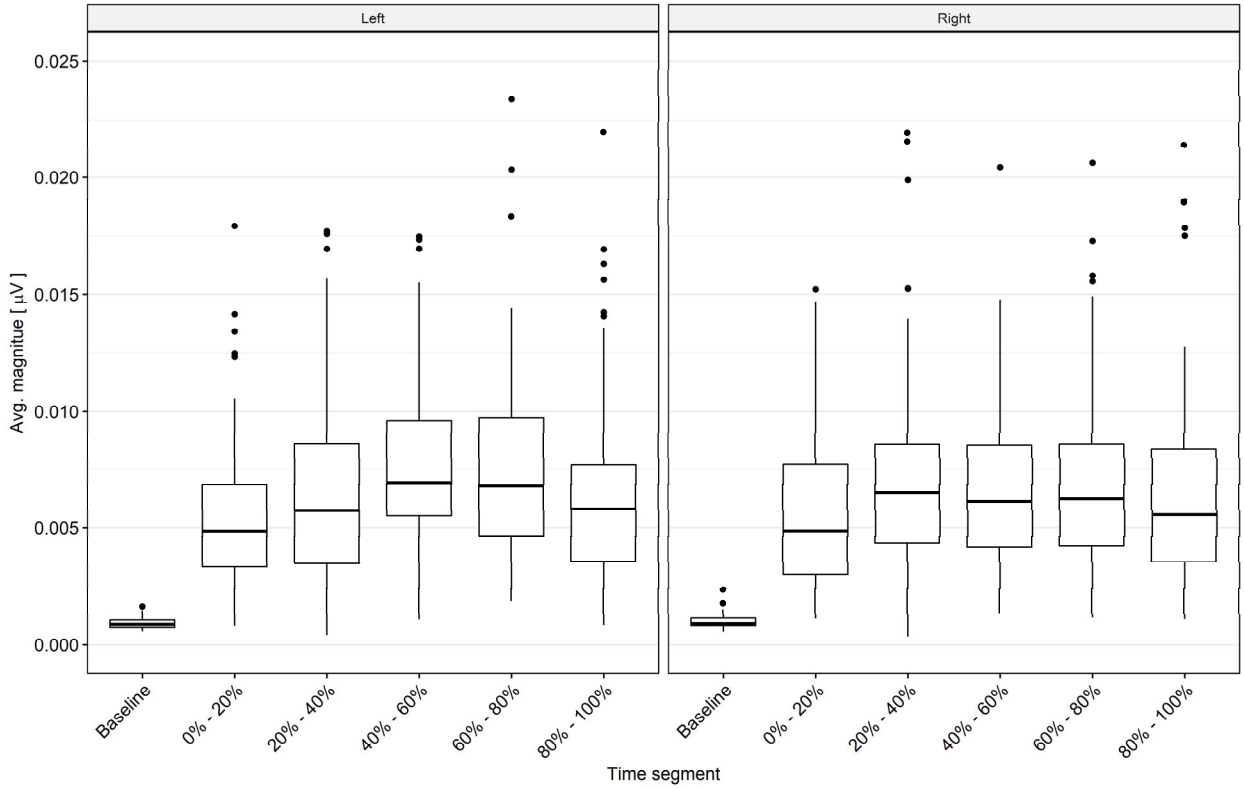

I

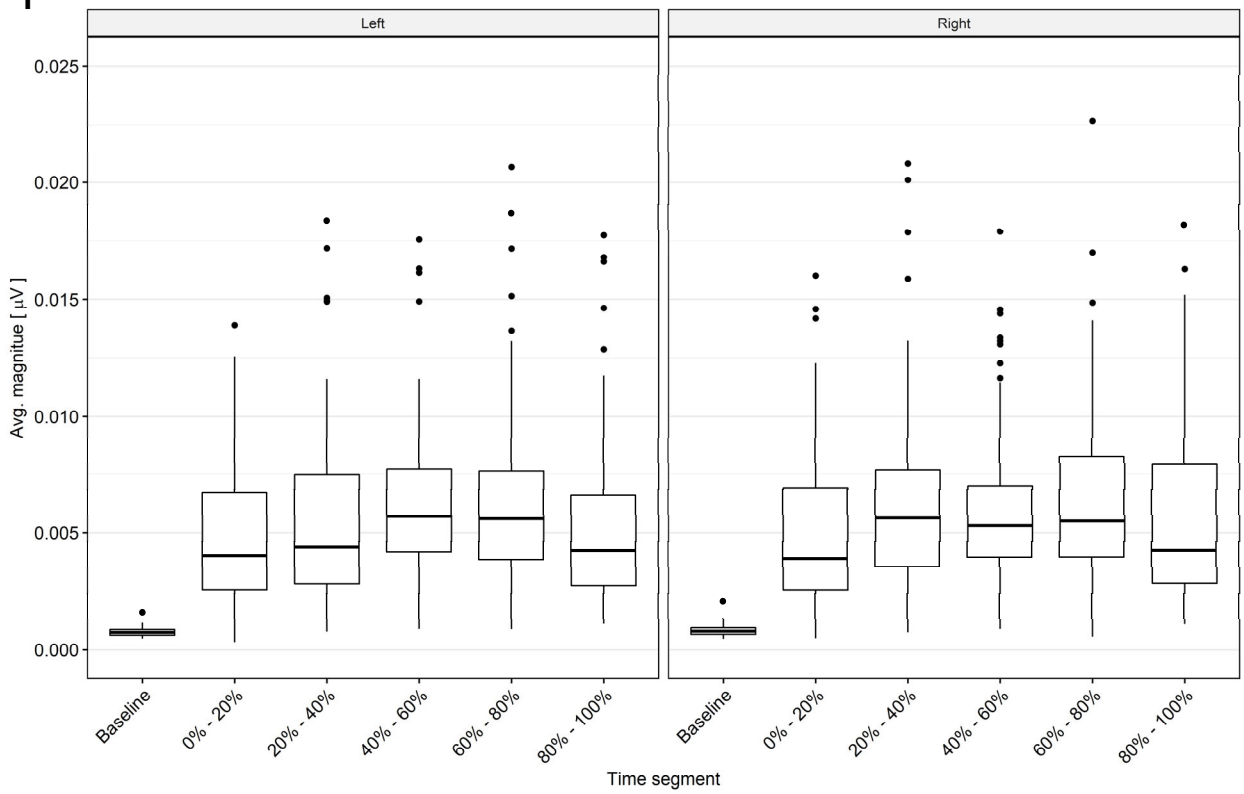
Thalamus
Left
Right
Avg. magnitue [µV]
0.025
0.020
0.015
0.010
0.005
0.000
Baseline
0% - 20%
20% - 40%
40% - 60%
60% - 80%
80% - 100%
Time segment

J

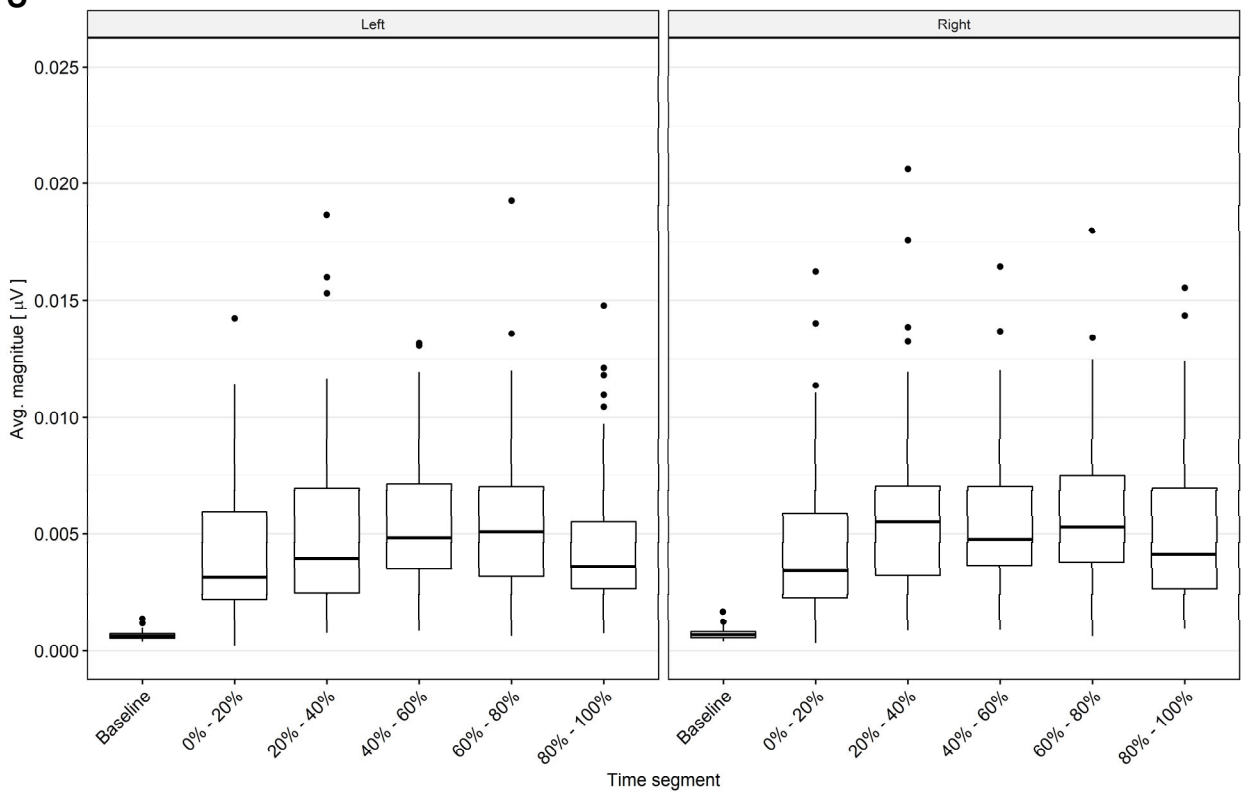
Lateral Ventricle
Left
Right
Avg. magnitue [µV]
0.025
0.020
0.015
0.010
0.005
0.000
Baseline
0% - 20%
20% - 40%
40% - 60%
60% - 80%
80% - 100%
Time segment

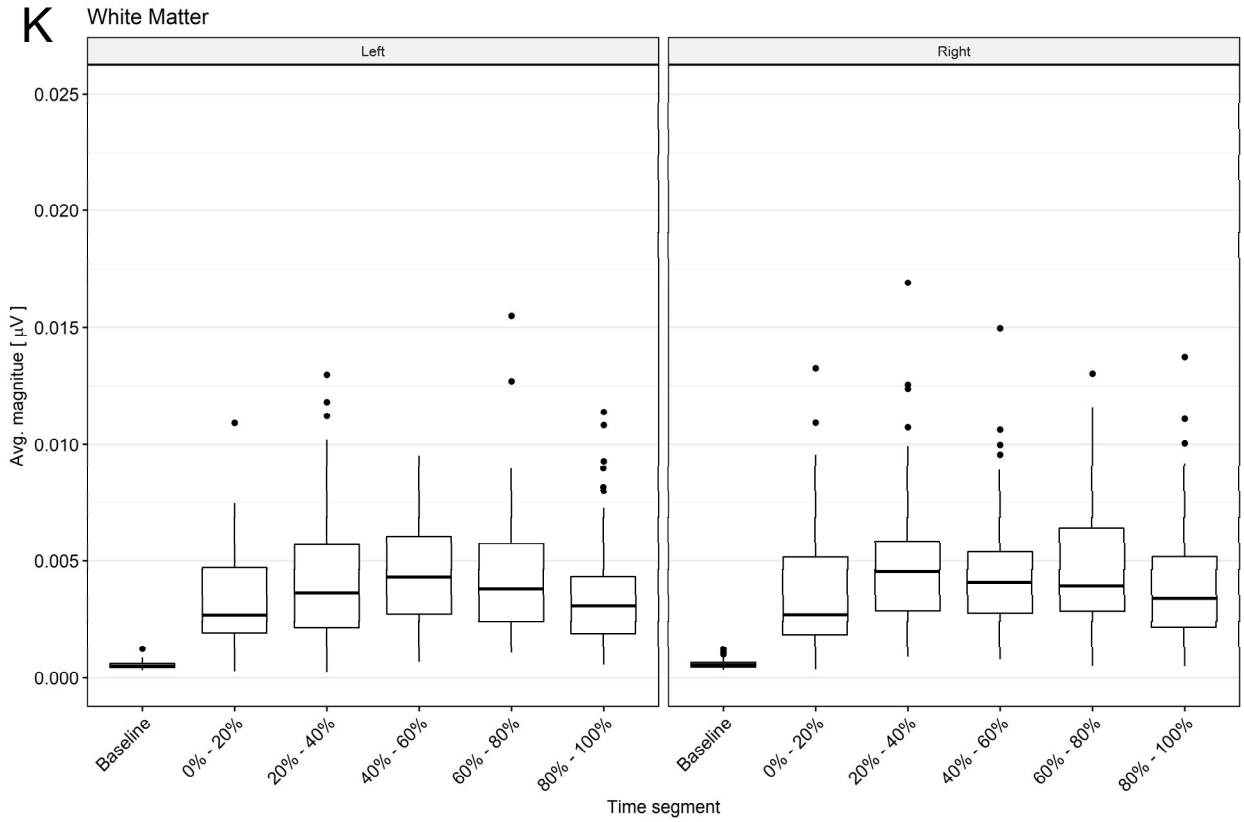

Supplementary figure 2. Source localization of the EEG in G1D. A-K. Temporal evolution of 81 seizure electrical activity patterns divided in 20% time intervals reflecting the current density magnitude changes in brain regions including accumbens, amygdala, caudate, cerebral cortex, ventral diencephalon, hippocampus, pallidum, putamen, thalamus, lateral ventricle and cerebral white matter. Baseline period is the time interval immediately prior to seizures. The time periods shown correspond to 0-20%, 20-40%, 40-60%, 60-80%, 80-100% segments within each of the 81 seizure episodes. Shown are average current densities averaged over all 81 episodes. Discrete points represent outlier values that fall more than 1.5 times the interquartile range above the third quartile.

[**Supplementary figure 3** below continues on the next 2 pages]

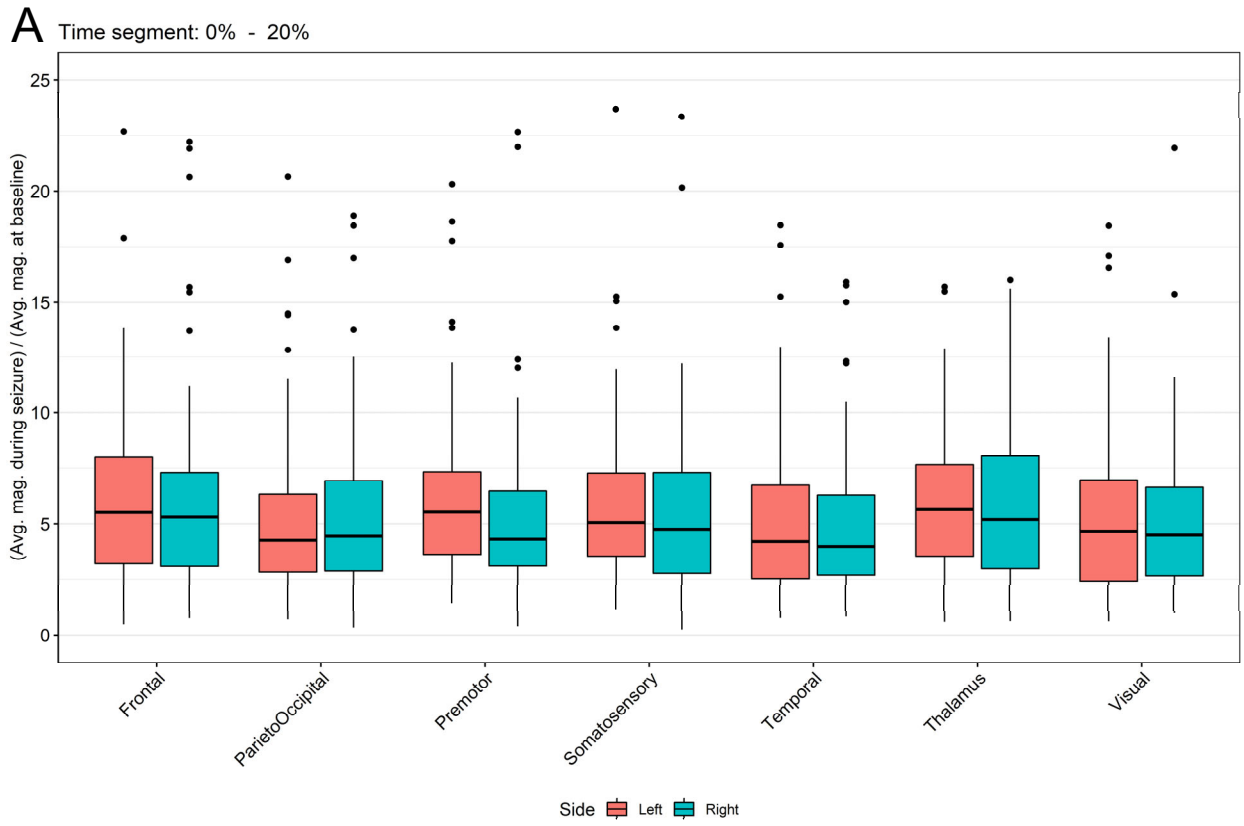

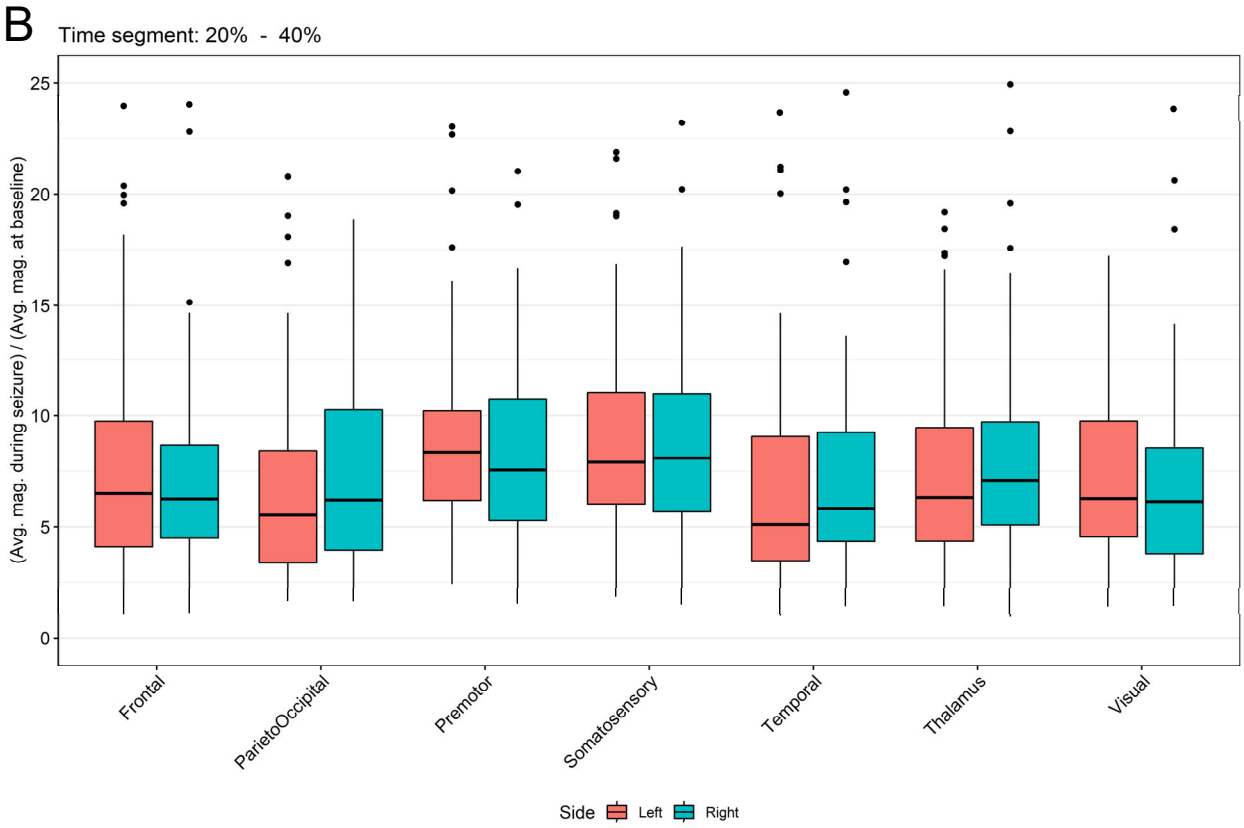

C Time segment: 40% - 60%

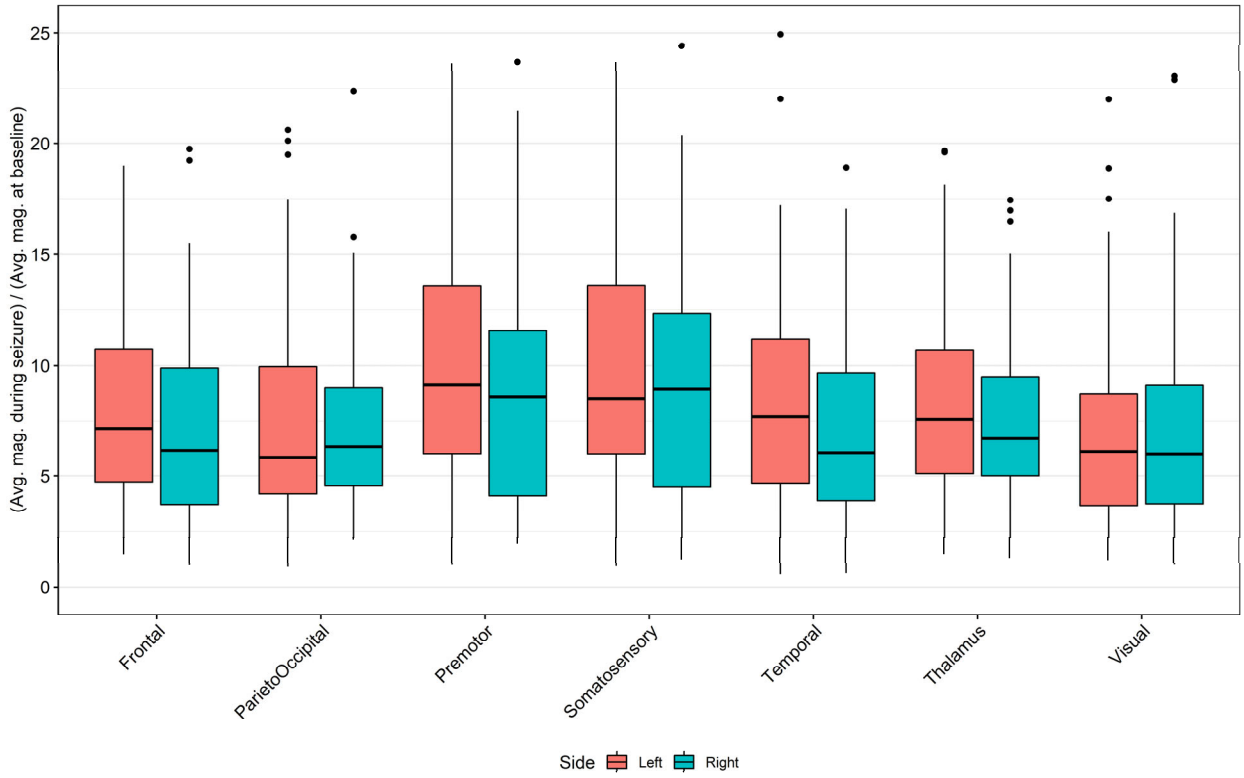

D Time segment: 60% - 80%

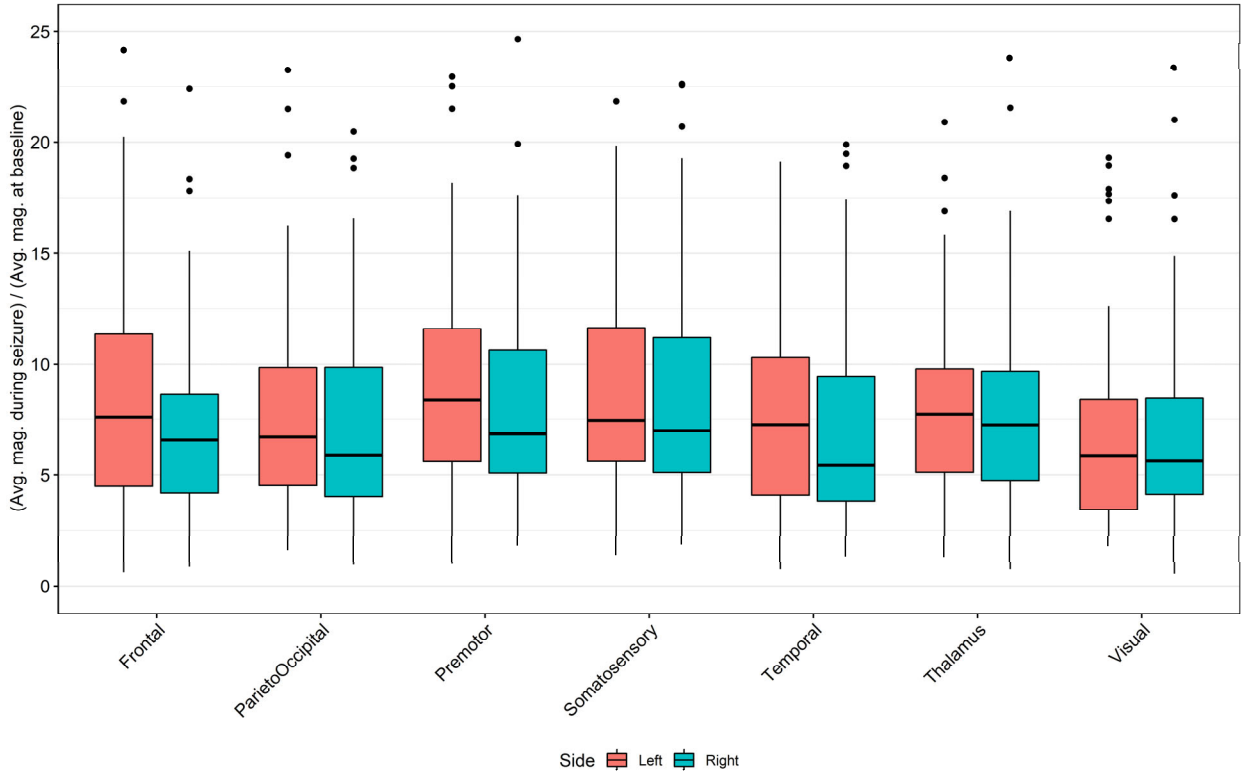

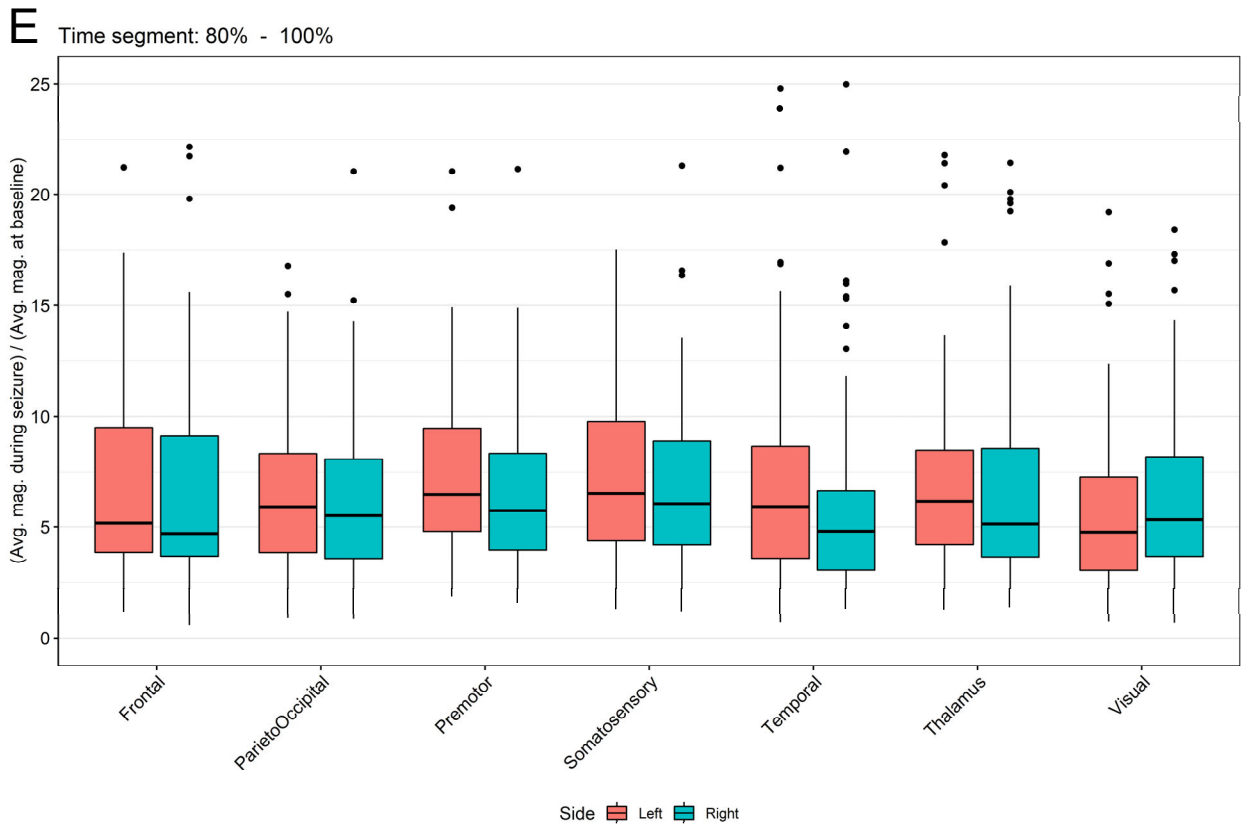

Supplementary figure 3. **Source localization of the EEG in G1D neocortex and thalamus**. A – E. Seizure electrical activity elevation over baseline in 6 cortical regions and thalamus during 20-40% of the seizure periods for each of the 81 seizure episodes. Shown are the ratios of current density averaged over 81 seizure episodes over that for baseline periods. Discrete points represent outlier values that fall more than 1.5 times the interquartile range above the third quartile.

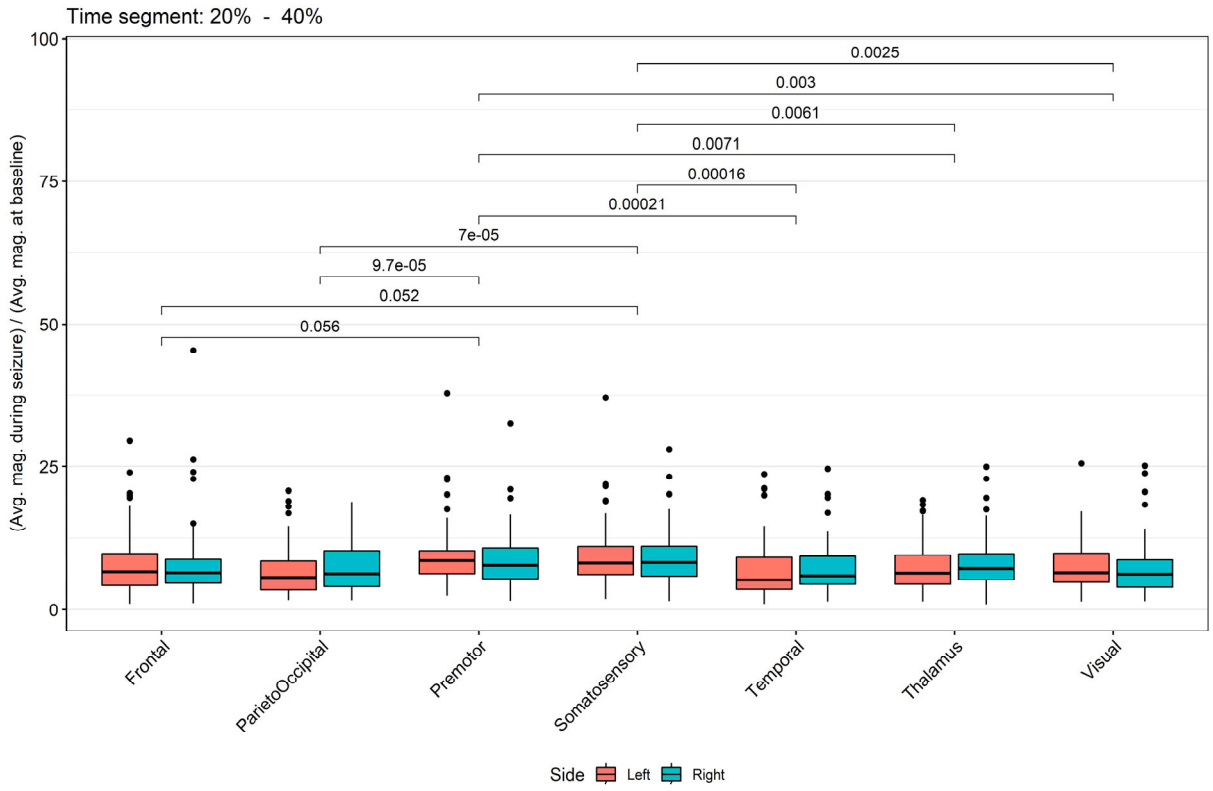

Supplementary figure 4. **Significance of regional comparisons for source localization of the EEG in G1D**. Comparisons of seizure activity elevation over baseline in each of the cortex regions and thalamus during 20-40% of the seizure intervals from 81 seizures. The numbers above the error bars are pairwise comparison p values. Discrete points represent outlier values that fall more than 1.5 times the interquartile range above the third quartile.

[**Supplementary figure 5** below continues on the next page]

A

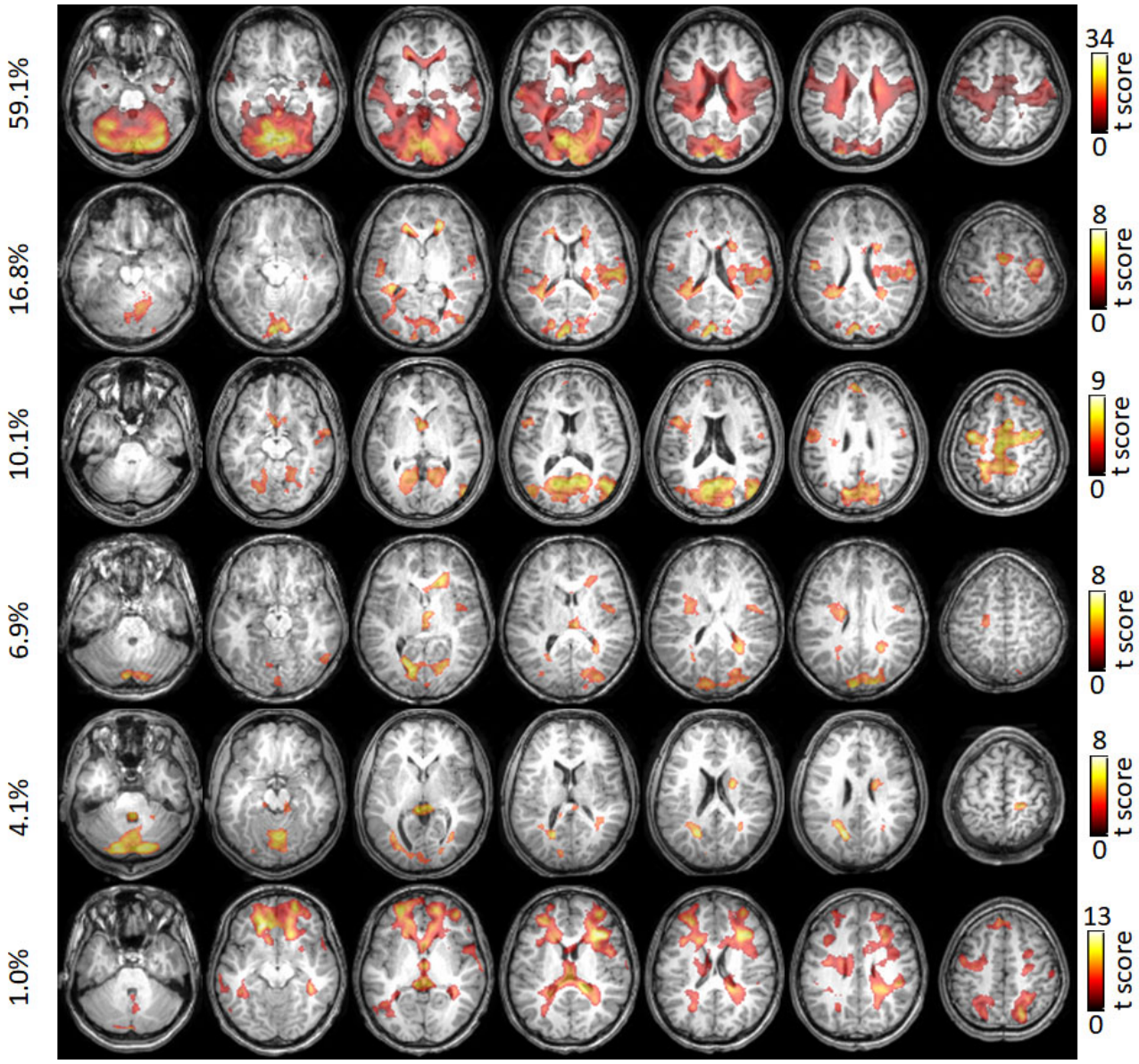

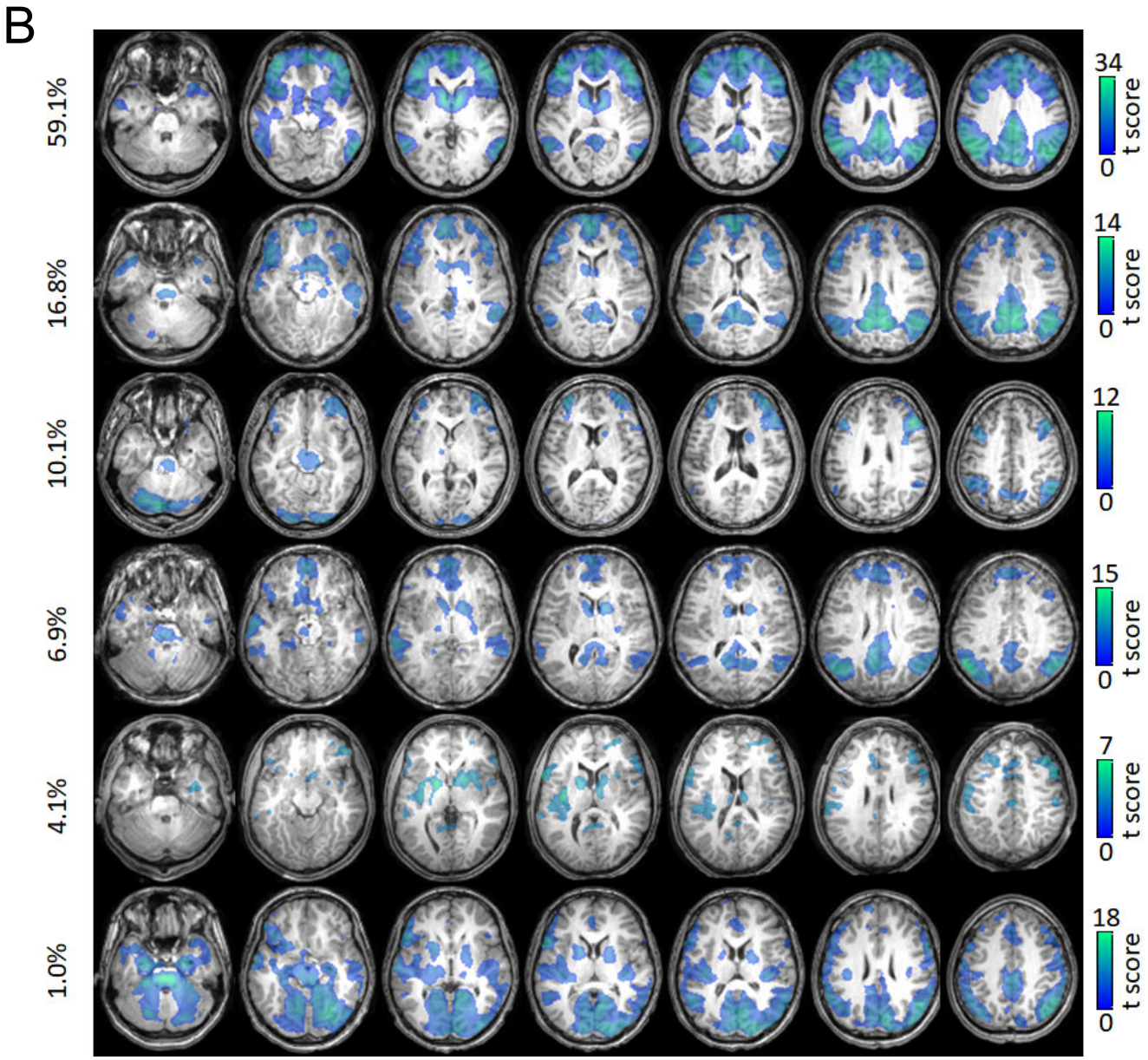

Supplementary figure 5. Simultaneous fMRI and EEG in 6 individuals with G1D. EEG traces obtained inside a 3T MRI scanner were utilized for manual correlation with changes in BOLD signal. Pulsation and eye blinking artifacts were removed. The individuals were instructed to remain awake and not directed to perform any tasks. Each participant is represented in a row of 7 T1 weighted images with superimposed changes in BOLD. The fraction of time occupied by seizures during the fMRI scan is given to the left for each individual in percent values. The coloring of the brain images and the rightmost scales indicate standard BOLD fMRI t values. A. Seizure-correlated increased or positive BOLD (orange-yellow color). B. Decreased or negative BOLD (blue-purple color). S fMRI scan duration was 15 min and T1 scan time was 4 min.

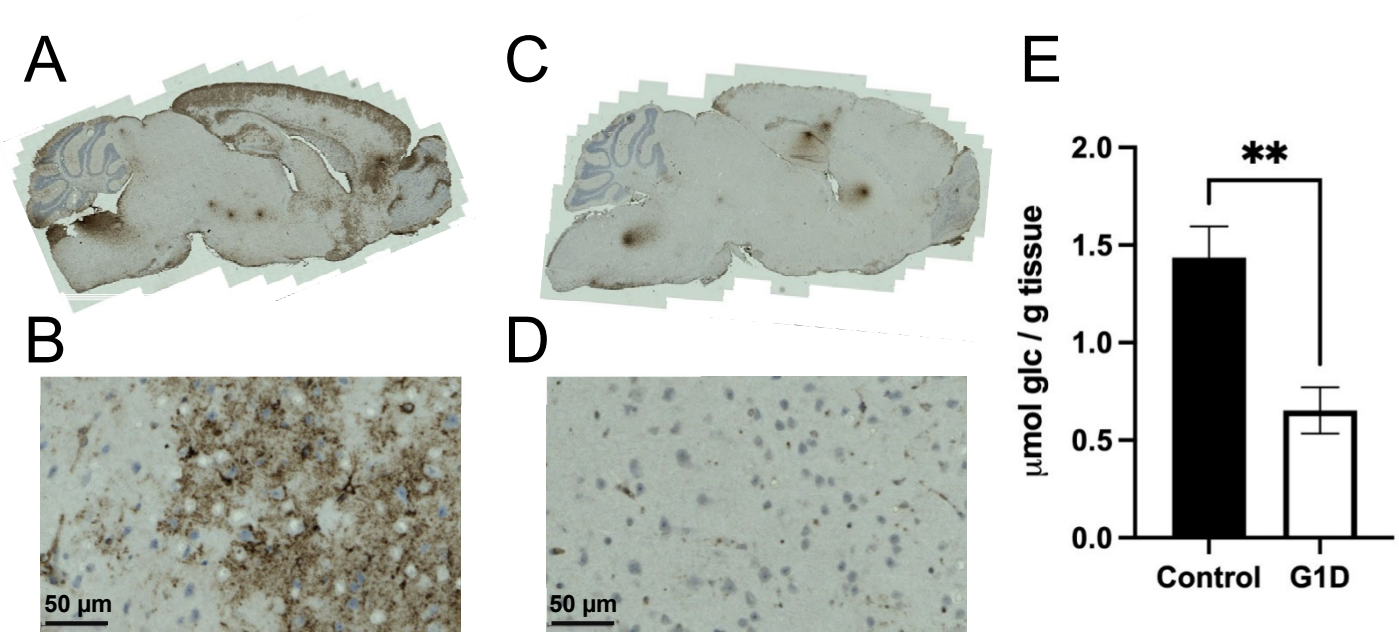

Supplementary figure 6. **Glycogen in the G1D brain**. A-D. Immunohistochemical staining with IV58B6 of parasagittal brain sections (n= 4 G1D and n= 4 control brains). A. Normal whole brain. C. G1D whole brain. B and D. Magnified cerebral cortex (occupying most of the right side of each panel) and associated white matter (remainder left side of each panel) staining in control (B) and G1D (D). E. Quantification of glycogen by amyloglucosidase assay in a spectrophotometric microplate reader in cerebellum expressed as the ratio of cerebral cortex glycogen content and total brain glycogen.

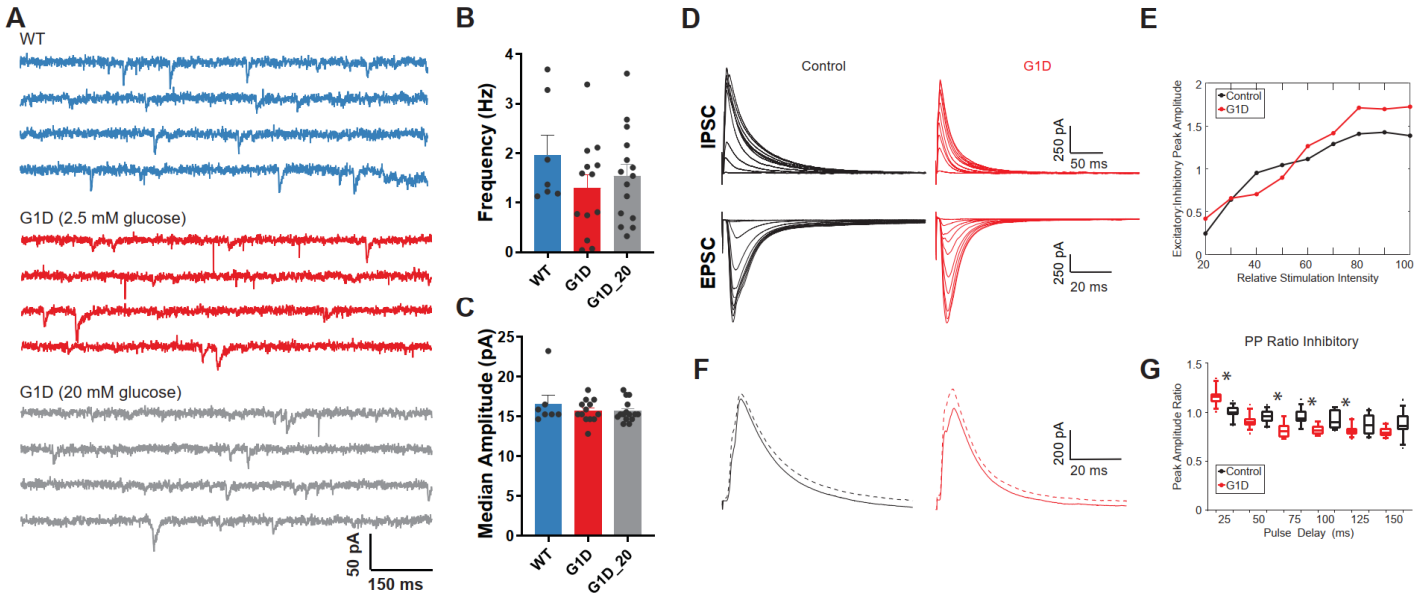

Supplementary figure 7. **Excitatory neurotransmission onto G1D cortical pyramidal neurons in G1D**. A. Voltage clamp recordings of mEPSCs in layer V pyramidal neurons in control (WT, blue) and G1D mice in 2.5 mM (red) or 20 mM glucose (green). Mean mEPSC (B) frequency and amplitude (C) in control and G1D group. D. Evoked IPSC and EPSC responses obtained from the same neuron following graded electrical afferent stimulation (control or WT, black and G1D, red). E. Stimulus-evoked differences in ratio of excitatory to inhibitory current amplitude in G1D (red) compared to control (WT, black) in layer V pyramidal neurons. F. Averaged current traces of IPSCs evoked in response to paired electrical stimulus (25 ms inter stimulus interval) of afferent fibers in G1D (red) compared to control (WT, black). G. Quantification of paired responses over a range of inter-stimulus intervals to display facilitation in G1D neurons at 25 ms inter-stimuli interval followed by a depressive response with inter-stimuli interval > 50 ms. * p< 0.05 compared to WT.

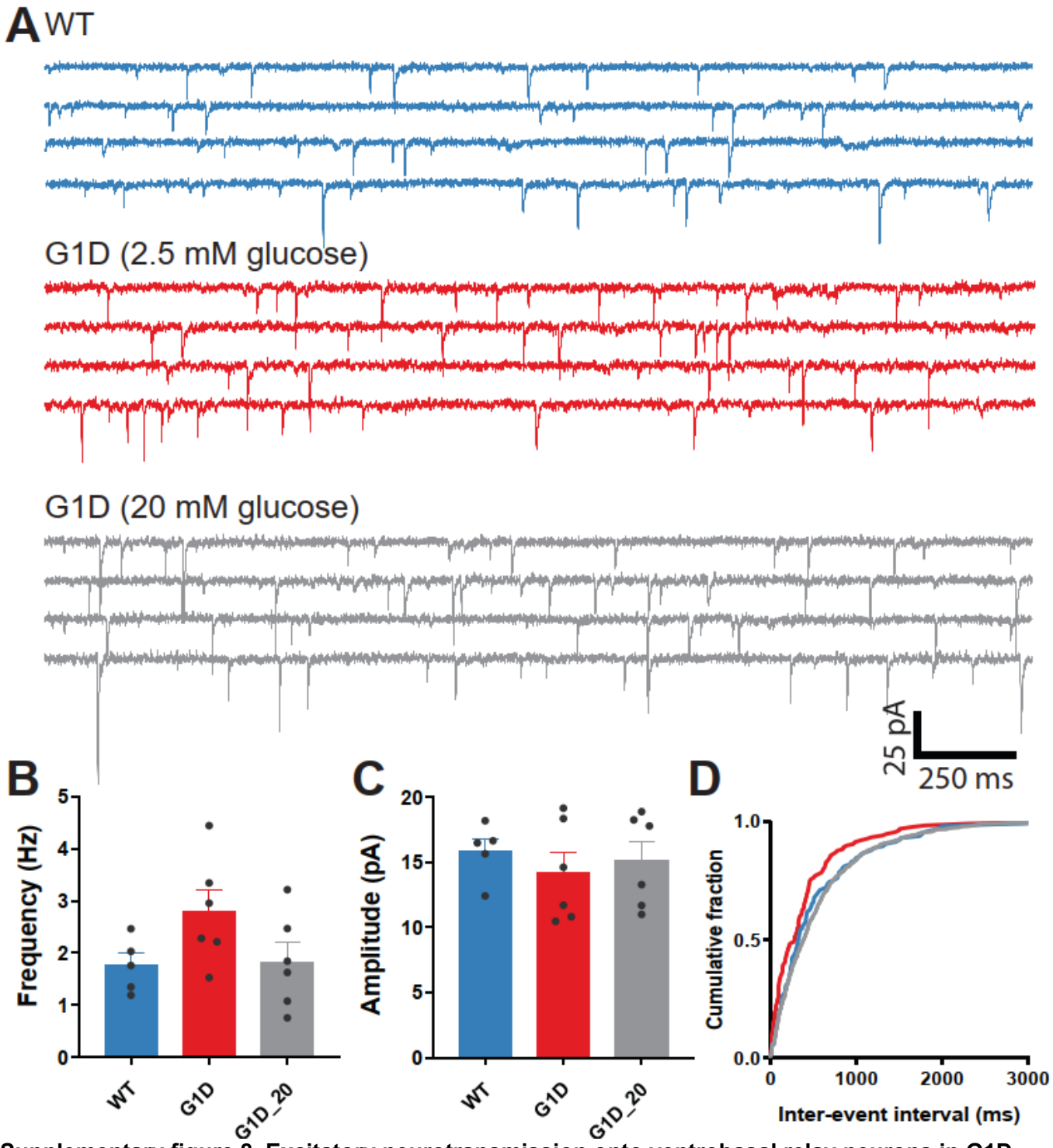

Supplementary figure 8. **Excitatory neurotransmission onto ventrobasal relay neurons in G1D**. A. Voltage clamp recordings of sEPSCs in VB relay neurons in control (WT, blue) and G1D mice (red, gray) in G1D brain slices perfused with 2.5 mM glucose. B, C. sEPSC frequency (B) and amplitude (C). D. Cumulative event probability in G1D neurons perfused with 2.5 mM glucose (red), and control (WT, blue) and G1D brain slices perfused with 20 mM glucose (gray).

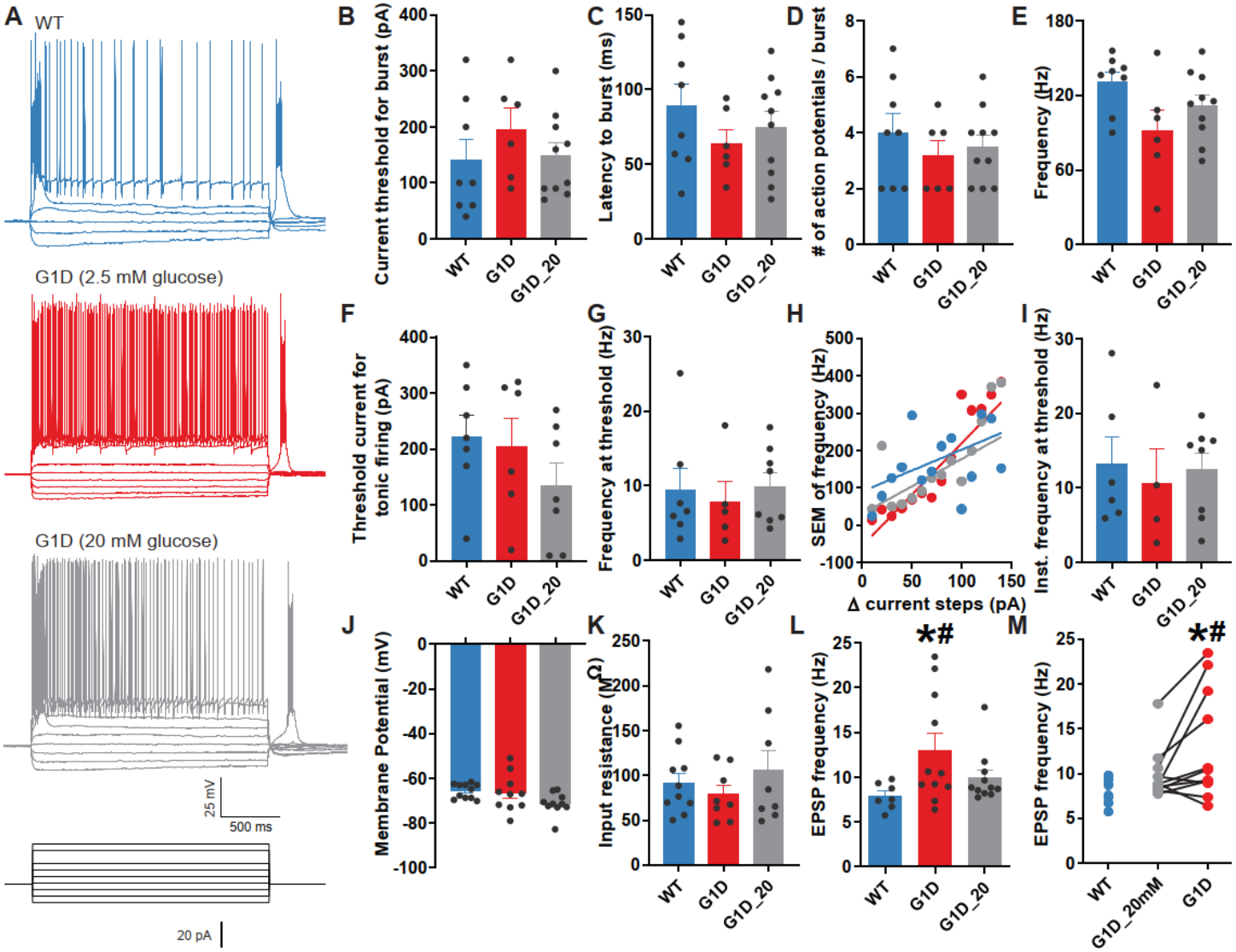

Supplementary figure 9. **Excitatory drive onto G1D ventrobasal neurons**. A. Current clamp traces from VB relay neurons of control (WT, blue), G1D in 2.5 mM glucose (red) and G1D in 20 mM glucose (gray) in response to depolarizing current steps. A postinhibitory rebound (PIR) following the end of hyperpolarizing current pulses is apparent in all three groups. B - E. Comparison of the 3 groups showing burst firing properties including (B) the threshold current need to evoke burst, (C) burst latency, (D) the number of action potentials per burst, and (E) burst firing frequency. F - I. Changes amongst the 3 groups showing tonic firing properties including (F) the threshold current for tonic firing, (G) threshold action potential frequency, (H) variation in frequency of tonic firing, and (I) instantaneous tonic firing frequency at threshold. J - M. Differences amongst the 3 groups in (J) resting membrane potential and (K) input resistance. L and M. Paired plots before and after perfusion of 2.5 mM glucose * $p < 0.05$ compared to WT (L) or G1D 20 mM glucose (M).

SUPPLEMENTARY TABLES

	Number of cells	Bursts per min	Events per burst	Burst duration (ms)	Interburst interval (ms)
G1D	5	20.32 ± 7.94	5.77 ± 0.50	78.45 ± 7.67	14932 ± 7017
Control	9	12.22 ± 4.98	4.90 ± 0.30	64.68 ± 5.00	19472 ± 6355

Table S1. Inhibitory postsynaptic current bursts in G1D and control neurons. $p > 0.05$, *t*-test with Welch correction for all four G1D to control wild type comparisons of burst properties.

	10 min	20 min	30 min	40 min	50 min
Percent sIPSC frequency change	100	91.53 ± 5.48	77.67 ± 7.25 *	81.21 ± 7.91 *	71.84 ± 10.35 *
Percent sIPSC amplitude change	100	94.76 ± 4.48	94.26 ± 4.18	97.31 ± 4.47	94.85 ± 5.15
Percent access resistance change	100	103 ± 1.87	94.40 ± 3.51	97.95 ± 1.34	90.23 ± 3.42

Table S2. **Spontaneous inhibitory postsynaptic currents in 5 control thalamocortical neurons under reduced glucose**. Percent change in sIPSC frequency, amplitude and cell access resistance measured at 10 min intervals, relative to values at 10 min. Perfusion was switched from 20 mM to 2.5 mM glucose at time 10 min. * $p < 0.05$ for changes relative to 10 min values, one-sample *t*-tests.

Datafile S1 – S3: raw data